

To appear in The Astronomical Journal

High Angular Resolution Observations at 7-mm of the Core of the Quadrupolar HH 111/121 Outflow

Luis F. Rodríguez

Centro de Radioastronomía y Astrofísica, UNAM, Morelia 58089, México

E-mail: l.rodriguez@astrosmo.unam.mx

José M. Torrelles

Instituto de Ciencias del Espacio (CSIC)-IEEC, Facultat de Física, Universitat de Barcelona, E-08028 Barcelona, Spain

E-mail: torrelles@ieec.fcr.es

Guillem Anglada

Instituto de Astrofísica de Andalucía (CSIC), Apartado 3004, E-18080 Granada, Spain

E-mail: guillem@iaa.es

Bo Reipurth

Institute for Astronomy, University of Hawaii, Hilo, HI, USA

E-mail: reipurth@ifh.hawaii.edu

Abstract. We present sensitive, high angular resolution ($0''.05$) VLA continuum observations made at 7 mm of the core of the HH 111/121 quadrupolar outflow. We estimate that at this wavelength the continuum emission is dominated by dust, although a significant free-free contribution ($\sim 30\%$) is still present. The observed structure is formed by two overlapping, elongated sources approximately perpendicular to each other as viewed from Earth. We interpret this structure as either tracing two circumstellar disks that exist around each of the protostars of the close binary source at the core of this quadrupolar outflow or a disk and a jet perpendicular to it. Both interpretations have advantages and disadvantages, and future high angular resolution spectroscopic millimeter observations are required to favor one of them in a more conclusive way.

1. Introduction

It is generally accepted that most stars form in binary or multiple systems (Lada & Lada 2003). Furthermore, in the case of low and intermediate-mass stars it is also known that the process occurs with the presence of an accretion disk and a collimated

outflow. From these two facts it follows that binary disk-jet systems should be common in regions of low-mass star formation. However, in practice these systems are hard to detect and identify and only a few have been studied in detail (e. g. Rodríguez et al. 1998; Anglada et al. 2004; Monin et al. 2007). Furthermore, it is still unclear if the members of a binary system will both be able to maintain the disks and outflows that characterize the formation of single stars. For example, the binary stars that form L1551 IRS5 are both believed to possess disks and jets (Rodríguez et al. 2003; Lim & Takakuwa 2006), while it is known that only one of the stars that forms the SVS 13 close binary system is associated with detectable circumstellar dust emission that is probably tracing a disk (Anglada et al. 2004).

One of the most interesting cases of a binary source that is known to exhibit independent outflows, most probably associated with each of the components of the binary, is HH 111 (Reipurth et al. 1999). Located in Orion at a distance of 414 pc (Menten et al. 2007), the optical HH 111 jet was discovered by Reipurth (1989). It is an extremely well-collimated jet, aligned approximately in the east-west direction (at a PA of $\sim 97^\circ$) and whose knots move in the plane of the sky with velocities of the order of several hundred km s^{-1} (Reipurth, Raga & Heathcote 1992). Reipurth, Bally & Devine (1997) found that this optical jet is part of a giant HH complex extending over 7.7 pc. This giant HH complex is very straight, suggesting great stability over the 10^4 years of its lifetime.

Near-infrared observations (Gredel & Reipurth 1993; 1994) revealed a second bipolar flow, named HH 121, that emerges from about the same position as the optical outflow, and is aligned approximately in the north-south direction (at a PA of $\sim 35^\circ$). This result suggested the presence of a close binary source in this region. Both the optical and the infrared outflows are detected as bipolar molecular outflows (Cernicharo & Reipurth 1996; Nagar et al. 1997; Lefloch et al. 2007).

At the center of the quadrupolar outflow is the source IRAS 05491+0247 = VLA 1, a suspected class I binary with a total luminosity of about $25 L_\odot$ (e.g. Stapelfeldt & Scoville 1993, Yang et al. 1997). To advance in our understanding of this source a high angular resolution image at millimeter wavelengths was needed to compare with the information available for the quadrupolar outflow.

2. Observations

The 7 mm continuum observations were made in the A configuration of the VLA of the NRAO‡, during 2006 February 10 and 15. The central frequency observed was 43.34 GHz and we integrated on-source for a total of approximately 5 hours. The absolute amplitude calibrator was 1331+305 (with an adopted flux density of 1.46 Jy) and the phase calibrator was 0552+032 (with a bootstrapped flux density of 0.84 ± 0.01 Jy and 0.89 ± 0.04 Jy, for the first and second epoch, respectively). The

‡ The National Radio Astronomy Observatory is operated by Associated Universities Inc. under cooperative agreement with the National Science Foundation.

phase noise rms was about 20° and 30° , for the first and second epoch, respectively, indicating good weather conditions. The phase center of the observations was at $\alpha(2000) = 05^h 51^m 46^s.25$; $\delta(2000) = +02^\circ 48' 29''.6$.

The data were acquired and reduced using the recommended VLA procedures for high frequency data, including the fast-switching mode with a cycle of 120 seconds. The effective bandwidth of the observations was 100 MHz.

3. Analysis

3.1. 7 mm Data

In Figure 1 we show the 7 mm image of the core of the HH 111/121 quadrupolar outflow. An unusual structure is evident in the image. The structure can be described as two overlapping, elongated sources aligned in the plane of the sky and approximately perpendicular to each other. We have fitted the emission with two Gaussian ellipsoids using the task JMFIT of the AIPS package (see Table 1). The data image and the model image are shown in Figure 2. In what follows, we will interpret this 7 mm structure, as well as that seen at 3.6 cm, in terms of combinations of ionized jet/dusty disk scenarios. However, other possibilities such as the presence of non-thermal components should be recognized.

For the purpose of comparison, we also show in Figure 1 the 3.6 cm continuum image obtained from the VLA data presented by Reipurth et al. (1999). These data have been recalibrated and the position of their phase calibrators updated by displacements of order $0''.16$ to the most recent values in the VLA calibrator catalog to allow accurate astrometric comparison with the 7 mm image. As first discussed by these authors, the 3.6 cm VLA image is suggestive of a quadrupolar jet, with a common origin within $0''.1$ (~ 40 AU). The main jet is aligned approximately in the east-west direction (that with a PA of $97^\circ \pm 1^\circ$ is taken to be the exciting agent of the extended optical HH 111 flow), while the second jet is aligned approximately in the north-south direction (that with a PA of $4^\circ \pm 4^\circ$ is taken to be the exciting agent of HH 121). The error in the position angle of the north-south jet was obtained from our reanalysis of the Reipurth et al. (1999) data. The quadrupolar structure of the 3.6 cm emission is more evident in the maximum entropy reconstruction of the image shown by Reipurth et al. (1999). From this image we crudely estimate that about 70% (0.7 ± 0.2 mJy) of the total 3.6 cm emission (1.0 mJy; see Table 2) comes from the east-west jet, while the remaining 30% (0.3 ± 0.2 mJy) comes from the weaker north-south jet.

We are then faced with a question: since the position angles of the two nearly perpendicular structures observed at 7 mm are similar to those observed at 3.6 cm, are we seeing at 7 mm two jets, two disks, or a jet and a disk? To address these interpretations, we first discuss additional continuum observations of the region.

3.2. Flux Densities at Other Wavelengths

We searched in the literature and in the VLA archives for additional data points of the continuum flux density of this source. In Table 2 we present a summary of the total flux densities obtained for the region. The observations are not taken simultaneously and if time variations are present, this will lead to an erroneous determination of the spectral indices. We also note that the observations are taken at different angular resolutions and that this may affect the comparison. The VLA is sensitive only to emission in angular scales smaller or comparable to ~ 25 times its angular resolution, while for OVRO the largest detectable angular scale is about 10 times the angular resolution. In particular, the 7 mm data was taken with the highest angular resolution (and thus the smallest detectable angular scale) and we may be underestimating the total flux density at this wavelength in comparison with the other observations, that are all taken at lower angular resolutions. Lower angular resolution VLA observations at 7 mm are needed to determine the complete flux density of HH 111.

The total continuum flux density at 7 mm is about 40% larger than the addition of the individual flux densities given in Table 1. This difference results from the presence of faint, extended 7 mm emission that is not accounted for in the individual Gaussian fits. Analysis of the residual (with the Gaussian fits removed) image suggests that this faint emission seems to extend over a diameter of $\sim 0''.3$, but its nature is unclear. As can be seen from Table 2 and in Figure 3, the flux density is relatively flat in the centimeter range and rises rapidly above ~ 30 GHz. We have fitted the data points with the sum of two power laws of the form:

$$S_\nu(\text{total}) = S_{8.4 \text{ GHz}}(\text{free} - \text{free})(\nu/8.4 \text{ GHz})^{0.3} + S_{43.3 \text{ GHz}}(\text{dust})(\nu/43.3 \text{ GHz})^{2.5},$$

where the first term is intended to represent the contribution of free-free emission from the ionized outflow and the second term is intended to represent the contribution of dust emission from the disks. Since we have four parameters to fit and only five data points, this fit is only intended to show that the data can be reasonably fitted with the sum of two power laws. In Figure 3 we show the fit for $S_{8.4 \text{ GHz}}(\text{free} - \text{free}) = 0.93$ mJy and $S_{43.3 \text{ GHz}}(\text{dust}) = 3.6$ mJy. Under this interpretation, the 8.44 GHz emission is clearly dominated by free-free, with only $\sim 6\%$ of dust contribution. On the other hand, the 43.34 GHz emission is dominated by dust, with a $\sim 30\%$ contribution from free-free. Following Rodríguez, Zapata, & Ho (2007) and Hunter et al. (2006), we estimate the total mass in the dust to be in the order of $0.1 M_\odot$. For this estimate a dust temperature of 45 K was used, following the assumptions of Stapelfeldt & Scoville (1993).

3.3. Two jets?

The excess of 7-mm emission with respect to the value expected from the extrapolation of the centimeter measurements rules out the possibility that at 7-mm we are simply observing two jets since we have estimated that a significant fraction ($\sim 70\%$) of the

7-mm emission is due to dust. However, we cannot fully rule out the possibility that we are seeing a core dominated by dust emission with the extended emission dominated by free-free emission.

3.4. Two disks?

This possible interpretation is suggested by the fact that at 3.6 cm the structure with the larger flux density is the east-west one, while at 7 mm this is true for the north-south structure (see Fig. 1 and Table 1). Rodríguez et al. (2008), from a comparison between the momentum rate in the molecular outflow and the radio continuum emission from the jet, have argued that high-mass young stars can be understood as a scaled-up version of low-mass young stars. Assuming that this conclusion is valid also for the parameters of jets and disks, and we tentatively assume that the flux density of disks and jets is correlated, this favors matching the east-west structure at 3.6 cm (the jet) with the north-south structure at 7 mm (the disk), and the north-south structure at 3.6 cm (the second jet) with the east-west structure at 7 mm (the second disk), forming a binary disk-jet system as that observed in L1551 IRS5 (Rodríguez et al. 2003).

This interpretation faces, however, three difficulties. The first difficulty is that the axes of the proposed disk-jet structures are not, as expected, nearly perpendicular. The east-west structure at 3.6 cm has a PA of $97^\circ \pm 1^\circ$, while the north-south structure at 7 mm has a PA of $23^\circ \pm 6^\circ$, having a relative angle of $74^\circ \pm 6^\circ$ between them. Furthermore, the north-south structure at 3.6 cm has a PA of $4^\circ \pm 4^\circ$, while the east-west structure at 7 mm has a PA of $116^\circ \pm 7^\circ$, having a relative angle of $112^\circ \pm 8^\circ$ between them.

The second difficulty is related to the stability of the proposed binary disk system. From Table 1, we estimate that the centroids of the two 7 mm structures are separated by $0''.036 \pm 0''.014$ or $\sim 15 \pm 6$ AU at a distance of 414 pc. We expect the disks in a binary system to be truncated at radii of order a fraction of the binary separation (Armitage, Clarke, & Tout 1999; Papaloizou & Pringle 1987; Pichardo, Sparke, & Aguilar 2005). We then expect the radii of the disks to be compact, ≤ 15 AU (assuming that the observed separation is comparable to the true separation). In contrast, the observed radii (see Table 1) are significantly larger, in the order of 35 AU.

The final difficulty is that, if we assume masses of order $1 M_\odot$ for the stars in the binary system, an orbital period of order 40 years is expected for a separation of ~ 15 AU. The expected timescale in which strongly misaligned binary disks should be brought into rough alignment by tidal torques is about 20 orbital periods (Bate et al. 2000), which is only 800 years if the 15 AU separation is real. With this relatively short timescale it is difficult to explain the lifetime of 10^4 years of the HH 111 jet and its remarkable stability over this period. On the other hand, it should be noted that Reipurth et al. (1992) have suggested that the separation of bright knots in the optical flow are consistent with a timescale of variation of the central source of 40 years.

These last two difficulties are mitigated if we consider that the real separation is much larger than the projected one. A physical separation of 105 AU would be consistent

with the values of 35 AU for tidally truncated radii. The orbital period would now be about 800 years and the timescale for alignment $\sim 1.6 \times 10^4$ years, consistent with the lifetime of the system. However, if we define the physical separation as r , the probability of observing it at a projected separation of r' or smaller is:

$$P(\leq r') = 1 - [1 - (r'/r)^2]^{1/2},$$

that for $r' = 15$ AU and $r = 105$ AU, gives $P(\leq r') \simeq 0.01$.

We conclude that either we are observing the binary at an unlikely orientation, that disks in binary systems are more stable and independent than previously thought, or that the interpretation is incorrect.

3.5. One jet and one disk?

This final interpretation implies that at 7-mm we are seeing a north-south structure dominated by dust emission that traces a disk and an east-west structure that could be related with the jet that powers the optical HH 111 outflow. A major advantage with this interpretation is that the structures have a relative angle of $93^\circ \pm 9^\circ$, very close to perpendicularity. The east-west structure has a flux density of 0.7 ± 0.2 mJy at 3.6 cm and of 1.4 ± 0.3 mJy at 7-mm. This results in a spectral index of 0.4 ± 0.2 , that is consistent with the value expected for a thermal jet (e. g. Anglada 1996; Eisloffel et al. 2000).

However, this interpretation also presents some difficulties. The east-west structure at 3.6 cm has a position angle of $97^\circ \pm 1^\circ$, while the east-west structure at 7 mm has a position angle of $116^\circ \pm 7^\circ$. In other words, the two structures are not nearly parallel, as expected if the 3.6 cm emission were the larger scale counterpart of the 7 mm jet emission. Under this interpretation, all the 7-mm emission is related to the HH 111 disk-outflow system and there is no evidence at this wavelength of the HH 121 system. Of course, it should be pointed out that the dust and free-free emission from the HH 121 system are probably present in the image at a low level but that we cannot disentangle their presence given the modest signal-to-noise ratio of the data.

4. Conclusions

Our main conclusions follow:

1) Our high angular resolution ($0''.05$) VLA continuum 7 mm observations of the core of the HH 111/121 quadrupolar outflow reveal a structure that can be described as two overlapping, elongated sources that appear approximately perpendicular to each other in the plane of the sky.

2) We discuss possible interpretations for this structure and conclude that the most viable ones are that we are observing two orthogonal disks around separate protostars or a disk with a perpendicular jet. Both interpretations have advantages and disadvantages, and high angular resolution spectroscopic millimeter observations (possible only in the

future with the Atacama Large Millimeter Array) are required to disentangle what is going on at the core of this quadrupolar outflow.

Acknowledgments

We thank an anonymous referee for valuable suggestions. LFR acknowledges the support of CONACyT, México and DGAPA, UNAM. JMT and GA are supported by the MEC AYA2005-05823-C03 grant (co-funded with FEDER funds). GA also acknowledges support from Junta de Andalucía.

References

- Anglada, G. 1996, in ASP Conf. Ser. 93, Radio Emission from the Stars and the Sun, ed. A. R. Taylor & J. M. Paredes (San Francisco: ASP), 3
- Anglada, G., Rodríguez, L. F., Osorio, M., Torrelles, José M., Estalella, R., Beltrán, M. T., & Ho, P. T. P. 2004, ApJ, 605, L137
- Armitage, P. J., Clarke, C. J., & Tout, C. A. 1999, MNRAS, 304, 425
- Bate, M. R., Bonnell, I. A., Clarke, C. J., Lubow, S. H., Ogilvie, G. I., Pringle, J. E., & Tout, C. A. 2000, MNRAS, 317, 773
- Cernicharo, J. & Reipurth, B. 1996, ApJ, 460, L57
- Eisloffel, J., Mundt, R., Ray, T. P., & Rodríguez, L. F. 2000, in Protostars and Planets IV, ed. V. Mannings, A. P. Boss, & S. S. Russell (Tucson: Univ. Arizona Press), 815
- Gredel, R. & Reipurth, B. 1993, ApJ, 407, L29
- Gredel, R. & Reipurth, B. 1994, A&A, 289, L19
- Hunter, T. R., Brogan, C. L., Megeath, S. T., Menten, K. M., Beuther, H., & Thorwirth, S. 2006, ApJ, 649, 888
- Lada, C. J., & Lada, E. A. 2003, ARA&A, 41, 57
- Lefloch, B., Cernicharo, J., Reipurth, B., Pardo, J. R., & Neri, R. 2007, ApJ, 658, 498
- Lim, J., & Takakuwa, S. 2006, ApJ, 653, 425
- Menten, K. M., Reid, M. J., Forbrich, J., & Brunthaler, A. 2007, A&A, 474, 515
- Monin, J.-L., Clarke, C. J., Prato, L., & McCabe, C. 2007, in Protostars and Planets V, ed. B. Reipurth, D. Jewitt, & K. Keil (Tucson: Univ. Arizona Press), p. 395
- Nagar, N.M., Vogel, S.N., Stone, J.M., & Ostriker, E.C. 1997, ApJ 482, L195
- Papaloizou, J. C. B., & Pringle, J. E. 1987, MNRAS, 225, 267
- Pichardo, B., Sparke, L. S., & Aguilar, L. A. 2005, MNRAS, 359, 521
- Reipurth, B. 1989, Nature, 340, 42
- Reipurth, B., Raga, A.C., & Heathcote, S. 1992, ApJ 392, 145
- Reipurth, B., Bally, J., & Devine, D. 1997, AJ, 114, 2708
- Reipurth, B., Yu, K. C., Rodríguez, L. F., Heathcote, S., & Bally, J. 1999, A&A, 352, L83
- Rodríguez, L. F. & Reipurth, B. 1994, A&A, 281, 882
- Rodríguez, L. F., D'Alessio, P., Wilner, D. J., Ho, P. T. P., Torrelles, J. M., Curiel, S., Gómez, Y., Lizano, S., Pedlar, A., Cantó, J., & Raga, A. C. 1998, Nature, 395, 355
- Rodríguez, L. F., Porras, A., Claussen, M. J., Curiel, S., Wilner, D. J., & Ho, P. T. P. 2003, ApJ, 586, L137
- Rodríguez, L. F., Zapata, L. A., & Ho, P. T. P. 2007, ApJ, 654, L143
- Rodríguez, L. F., Moran, J. M., Franco-Hernández, R., Garay, G., Brooks, K. J. & Mardones, D. 2008, AJ, 135, 2370
- Stapelfeldt, K., Scoville, N.Z. 1993, ApJ, 408, 239
- Yang, J., Ohashi, N., Yan, J., Liu, C., Kaifu, N., & Kimura, H. 1997, ApJ 475, 683

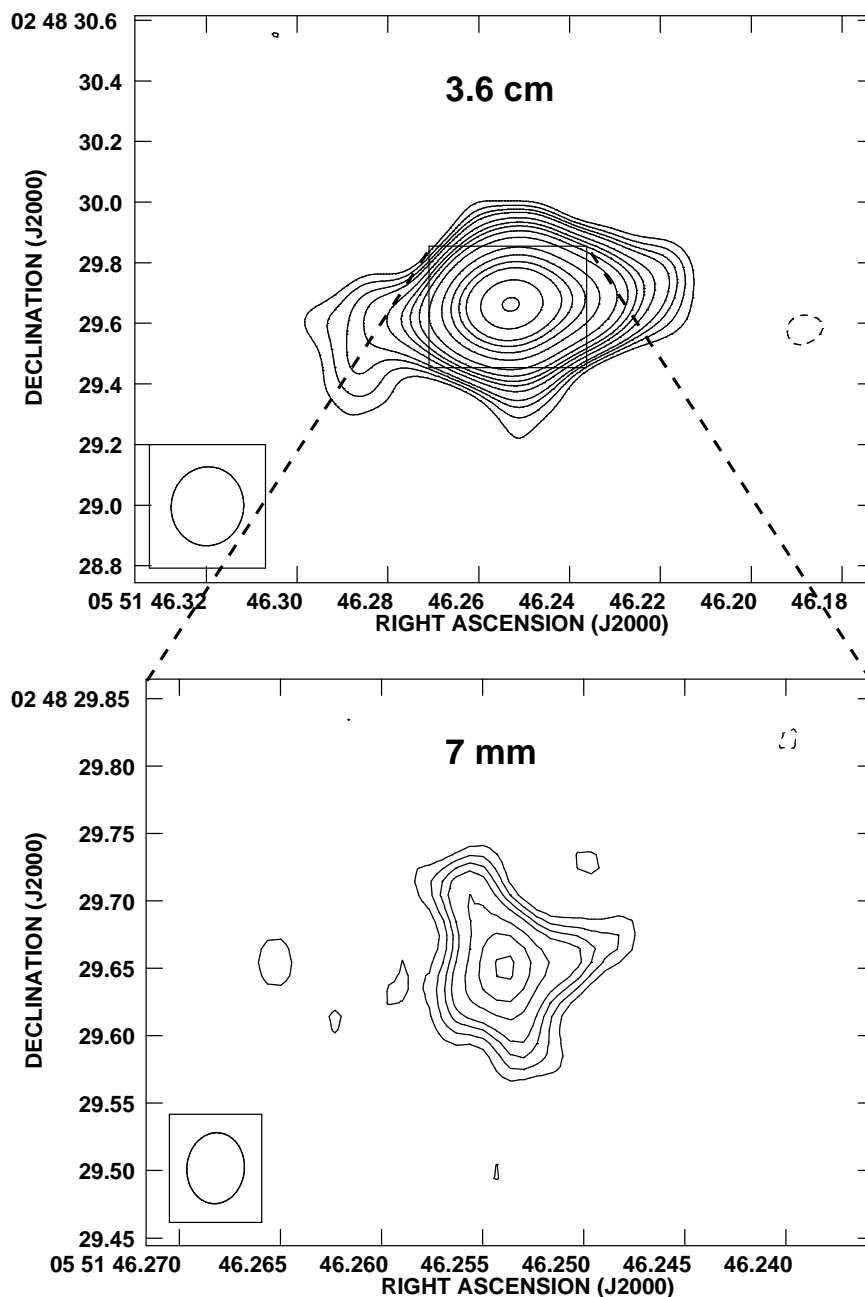


Figure 1. Top: Contour image of the 3.6 cm continuum emission from the core of the HH111/121 quadrupolar outflow, made from the data of Reipurth et al. (1999). Contours are $-4, -3, 3, 4, 5, 6, 8, 10, 12, 15, 20, 30, 40, 50, 60, 80$ and 100 times $4.8 \mu\text{Jy beam}^{-1}$, the rms noise of the image. The half power contour of the synthesized beam ($0''.26 \times 0''.24$ with a position angle of -8°) is shown in the bottom left corner. The rectangle marks the region shown in the 7 mm image (see below). Bottom: Contour image of the 7 mm continuum emission from the core of the HH111/121 quadrupolar outflow. Contours are $-4, -3, 3, 4, 5, 6, 8, 10,$ and 12 times $56 \mu\text{Jy beam}^{-1}$, the rms noise of the image. The half power contour of the synthesized beam ($0''.053 \times 0''.043$ with a position angle of -5°) is shown in the bottom left corner. Both images were made with the ROBUST parameter of IMAGR set to 0.5.

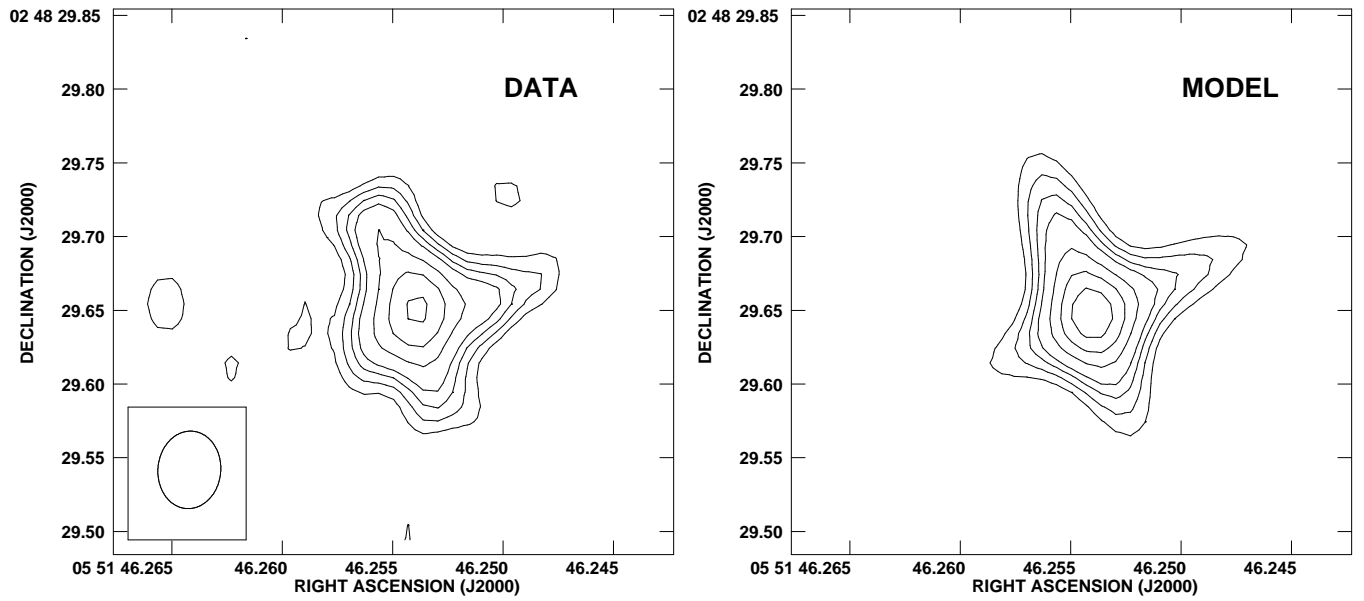


Figure 2. Contour images of the 7 mm continuum emission (left) and of the model with two Gaussian ellipsoids. Contours are -4, -3, 3, 4, 5, 6, 8, 10, and 12 times $56 \mu\text{Jy beam}^{-1}$, the rms noise of the image. The half power contour of the synthesized beam ($0''.053 \times 0''.043$ with a position angle of -5°) is shown in the bottom left corner of the data image.

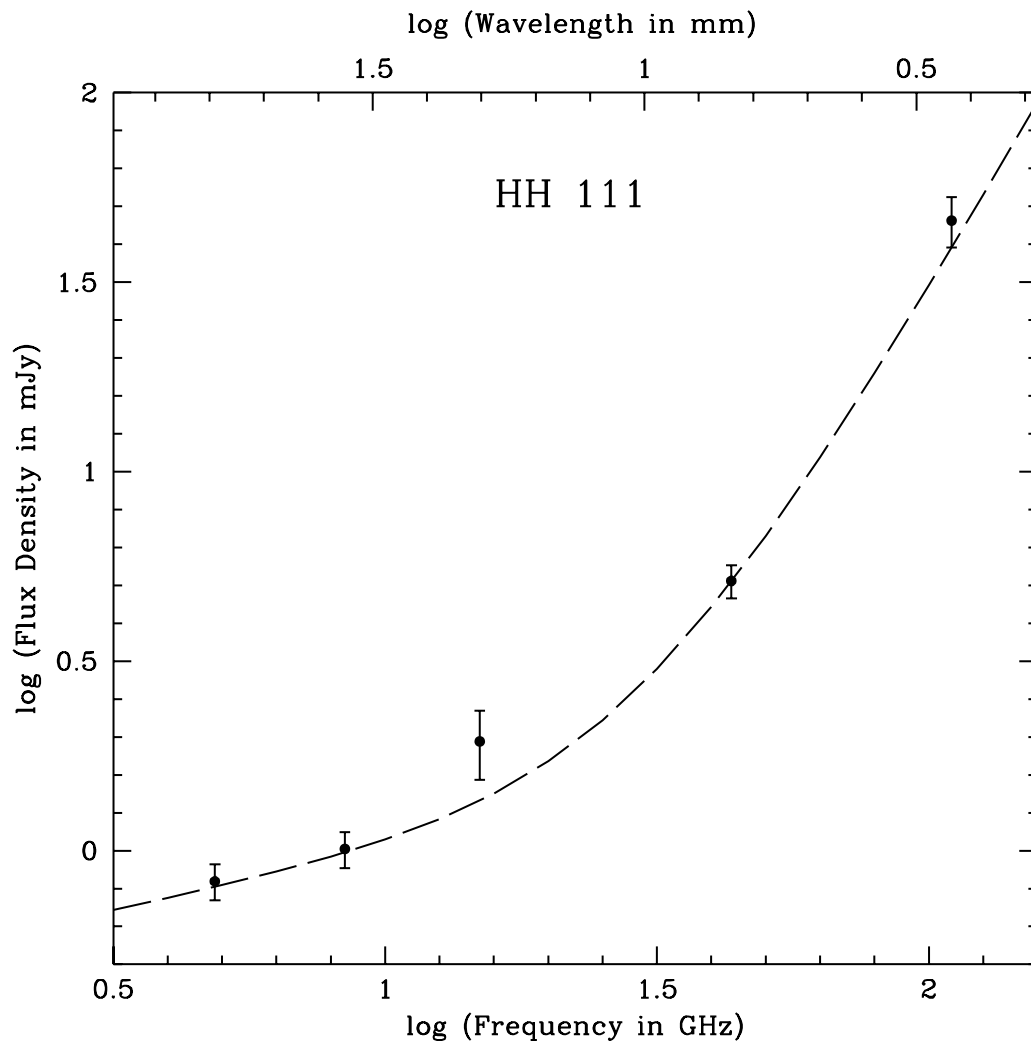


Figure 3. Continuum data points for the core of the HH 111/121 quadrupolar outflow, from Table 2. The dashed line is the fit described in the text.

Table 1. Decomposition of the 7 mm Continuum Emission in Two Components.

Component	$\alpha(\text{J2000})^a$	$\delta(\text{J2000})^a$	Total Flux Density (mJy)	Deconvolved Angular Size ^b
North-South	05 51 46.2545	02 48 29.660	2.2 ± 0.3	$0''.15 \pm 0''.02 \times 0''.05 \pm 0''.01; + 23^\circ \pm 6^\circ$
East-West	05 51 46.2521	02 48 29.659	1.4 ± 0.3	$0''.20 \pm 0''.05 \times \leq 0''.04; + 116^\circ \pm 7^\circ$

^a Units of right ascension are hours, minutes, and seconds and units of declination are degrees, arcminutes, and arcseconds. Absolute positional accuracy is estimated to be $0''.01$.

^b Major axis \times minor axis; position angle of major axis.

Table 2. Total Flux Densities for the Core of the HH 111/121 Quadrupolar Outflow.

Frequency (GHz)	Flux Density (mJy)	VLA Configuration	Angular Resolution (")	VLA Project Code	Epoch of Observation	
4.86	0.83±0.09	CnB	~4.0	AA183	1994 Sep 21	
8.44	1.01±0.11	A	~0.25	AR277/8	1992 Nov 02 + 1994 Apr 30	F
14.94	1.94±0.40	D	~5.7	AR241	1991 May 17	Rodri
43.34	5.15±0.52	A	~0.05	AT325	2006 Feb 10+15	
110.2	46.0±7.0	- ^b	~7.0	- ^b	1989 Dec - 1990 May	Stap

^a Flux densities from our analysis of the data.

^b Data taken with the Owens Valley Radio Observatory Millimeter Interferometer.